

SECULAR EVOLUTION VIA BAR-DRIVEN GAS INFLOW: RESULTS FROM BIMA SONG

KARTIK SHETH,^{1,2,3} STUART N. VOGEL,² MICHAEL W. REGAN,^{3,4} MICHELE D. THORNLEY,⁵ AND PETER J. TEUBEN²

Received 2004 December 7; accepted 2005 May 18

ABSTRACT

We present an analysis of the molecular gas distributions in the 29 barred and 15 unbarred spirals in the BIMA CO ($J = 1-0$) Survey of Nearby Galaxies (SONG). For galaxies that are bright in CO, we confirm the conclusion by Sakamoto et al. that barred spirals have higher molecular gas concentrations in the central kiloparsec. The SONG sample also includes 27 galaxies below the CO brightness limit used by Sakamoto et al. Even in these less CO-bright galaxies we show that high central gas concentrations are more common in barred galaxies, consistent with radial inflow driven by the bar. However, there is a significant population of early-type (Sa–Sbc) barred spirals (6 of 19) that have no molecular gas detected in the nuclear region and have very little out to the bar corotation radius. This suggests that in barred galaxies with gas-deficient nuclear regions, the bar has already driven most of the gas within the bar corotation radius to the nuclear region, where it has been consumed by star formation. The median mass of nuclear molecular gas is over 4 times higher in early-type bars than in late-type (Sc–Sdm) bars. Since previous work has shown that the gas consumption rate is an order of magnitude higher in early-type bars, this implies that the early types have significantly higher bar-driven inflows. The lower accretion rates in late-type bars can probably be attributed to the known differences in bar structure between early and late types. Despite the evidence for bar-driven inflows in both early and late Hubble-type spirals, the data indicate that it is highly unlikely for a late-type galaxy to evolve into an early type via bar-induced gas inflow. Nonetheless, secular evolutionary processes are undoubtedly present, and pseudobulges are inevitable; evidence for pseudobulges is likely to be clearest in early-type galaxies because of their high gas inflow rates and higher star formation activity.

Subject heading: galaxies: evolution — galaxies: nuclei — galaxies: spiral — galaxies: starburst — galaxies: structure — ISM: molecules

1. INTRODUCTION

Nearly three-quarters of all nearby disk galaxies have a bar (Eskridge et al. 2000; Menéndez-Delmestre et al. 2004); recent studies suggest that the bar fraction remains high at $z > 0.7$ (Sheth et al. 2003) and is perhaps constant to a redshift of 1 (Elmegreen & Elmegreen 2004; Jogee et al. 2004). Models show that the nonaxisymmetric bar potential induces large-scale streaming motions in the stars and gas (Sellwood & Wilkinson 1993 and references therein; Athanassoula 1992a, 1992b). This mixing is responsible for the shallower chemical abundance gradients observed in barred spirals compared to unbarred spirals (Vila-Costas & Edmunds 1992; Zaritsky et al. 1994; Martin & Roy 1994; Martinet & Friedli 1997). Studies of gas kinematics in the bar indicate that molecular gas is flowing inward down the bar dust lanes (Downes et al. 1996; Regan et al. 1999; Sheth et al. 2000, 2002). Enhancement of the star formation activity in the nuclei of barred spirals (e.g., Sérsic & Pastoriza 1967; Hawarden et al. 1986; Ho et al. 1997) suggests that either the conditions at the centers of barred spirals are more favorable for star formation or these regions have a higher gas content. We note that the enhancement in star formation activity is primarily

found in early Hubble-type barred spirals (Ho et al. 1997). Ho et al. divide the galaxies with the Hubble types Sa–Sbc as early types and galaxies with type Sc–Sdm as late types; we use this division throughout the remainder of this paper (see also § 2). The observational results noted above provide indirect observational evidence that bars transport gas toward their centers.

Models also suggest that further inflow of gas by a “bars-within-bars” scenario may fuel active galactic nuclei (Shlosman et al. 1989), although the evidence for such fueling is weak (Regan & Mulchaey 1999; Knapen et al. 2000; Laine et al. 2002; Laurikainen et al. 2004). Other studies have suggested that bar-induced gas inflows may lead to the formation of new (pseudo) bulges (e.g., Kormendy 1993; see also the recent review by Kormendy & Kennicutt 2004) and evolve late Hubble-type spirals into early Hubble types (e.g., Friedli & Benz 1995; Kenney 1996; Zhang 1999). The most dramatic prediction is that bars may destroy themselves if they accumulate sufficient mass at their centers (Pfenniger & Norman 1990; Friedli & Benz 1993; Norman et al. 1996; Bournaud & Combes 2002; Athanassoula 2003; Shen & Sellwood 2004; see also the review by Kormendy & Kennicutt 2004 and references therein).

Starburst activity, the formation of a pseudobulge, secular evolution of a galaxy along the Hubble sequence, and the destruction of the bar are all expected to occur when gas accretes in the nuclear region of a galaxy. Is there any direct evidence for excess gas at the center of barred spirals? While studies of individual galaxies have shown that at least some bars have a substantial amount of molecular gas near their centers (e.g., Kenney 1996; Turner 1996), only one study has addressed the issue of whether the central regions of barred spirals are *systematically* more gas-rich than those in unbarred spirals. With a sample of 20 (10 barred and 10 unbarred) galaxies, the Nobeyama Radio Observatory–Owens

¹ Spitzer Science Center, Mail Stop 220-6, California Institute of Technology, Pasadena, CA 91125; kartik@astro.caltech.edu.

² Department of Astronomy, University of Maryland, College Park, MD 20742-2421.

³ Visiting Astronomer, Kitt Peak National Observatory, National Optical Astronomy Observatory, which is operated by the Association of Universities for Research in Astronomy, Inc., under cooperative agreement with the National Science Foundation (NSF).

⁴ Space Telescope Science Institute, 3700 San Martin Drive, Baltimore, MD 21218.

⁵ Department of Physics, Bucknell University, Lewisburg, PA 17837.

Valley Radio Observatory (NRO-OVRO) survey (Sakamoto et al. 1999a) found that the central concentration (f_{con}), defined as the ratio of the nuclear molecular gas surface density (Σ_{nuc}) to the total (disk-averaged) molecular gas surface density (Σ_{tot}), is significantly higher in barred spirals than unbarred spirals (Sakamoto et al. 1999b). While f_{con} increases when gas is transported to the center, it decreases when gas is consumed by circumnuclear star formation. Since barred spirals have elevated circumnuclear star formation activity (e.g., Sérsic & Pastoriza 1967; Hawarden et al. 1986; Ho et al. 1997), a priori one expects *lower* f_{con} -values in barred spirals, *unless there is a fresh influx of molecular gas*. Thus, a higher f_{con} -value in barred spirals than unbarred spirals is strong evidence for bar-induced gas inflow and accumulation. Moreover, f_{con} is robust against biases in galaxy size, mass, and distance. In addition, given the shallower metallicity gradients typically found in barred spirals, variations in CO brightness with metallicity would cause f_{con} to be *smaller* in barred than unbarred spirals, the opposite of what is observed (Ho et al. 1997).

Although the NRO-OVRO result is statistically significant, the sample size is modest (20 galaxies) and consists of CO-bright galaxies.⁶ The NRO-OVRO sample has only four galaxies of Hubble type Sc or later. Hence, it is unclear whether the observed difference in f_{con} between barred and unbarred spirals is representative of all spiral galaxies. Does this result extend to CO-faint spirals? How does it vary with Hubble type? Is there any evidence for secular evolution from late to early Hubble type?

With the larger and more diverse sample of spiral galaxies in SONG, we can address these outstanding questions. SONG contains 3 times as many bars as the NRO-OVRO study and 50% more unbarred spirals. There are 27 galaxies in SONG with lower CO brightness than those in the NRO-OVRO sample because SONG galaxies were chosen based on an apparent optical magnitude instead of CO brightness. Moreover, SONG has 15 spirals of Hubble type Sc–Sd; thus, we can directly evaluate the influence of bars on late Hubble-type spirals. One other advantage of SONG is that it imaged the CO emission over the entire bar region in all but one of the barred spirals; hence, we can compare the gas distribution in the central region to the available gas in the bar and place the observations in the context of secular evolution.

2. OBSERVATIONS, DATA REDUCTION, AND ANALYSIS

In SONG, the molecular gas distributions (using the CO $J = 1-0$ line) in 44 nearby spirals (Sa–Sd) were mapped with the Berkeley-Illinois-Maryland Association (BIMA) interferometer (Welch 1996) and the NRAO⁷ 12 m single-dish telescope at Kitt Peak. The SONG sample galaxies are listed in Table 1. The details of the survey and properties of the sample are described in greater detail in Helfer et al. (2003; in particular see § 2.2). In some cases the distances and position angles used by us are different than those noted by Helfer et al. (2003); we used the most recent measurements from the literature. We note that we checked the results of our study with the Helfer et al. distances and position angles and found no systematic differences, and the results from this study remain unchanged. The selection criteria for the SONG sample were heliocentric velocity $V_{\text{Hel}} < 2000 \text{ km s}^{-1}$, declination $\delta > -20^\circ$, inclination $i < 70^\circ$, and apparent magnitude

$B_T < 11$. This leads to a sample that is representative of disk galaxies in the local universe.

The typical data cube has a synthesized beam of $6''$ and a field of view of $3'$. In a 10 km s^{-1} channel the typical noise is $\sim 58 \text{ mJy beam}^{-1}$. The measured fluxes are accurate to 15%; uncertainties are due to the absolute amplitude calibration. The galaxy centers are obtained from the 2MASS Large Galaxy Survey (Jarrett et al. 2003).

With the BIMA SONG data, we measure the molecular gas mass (M_{nuc}) and surface density (Σ_{nuc}) in the central kiloparsec using standard routines in MIRIAD (Sault et al. 1995); we discuss why we chose the central kiloparsec at the end of this section. We use the FCRAO or the NRAO 12 m SONG data for the total molecular gas mass (M_{tot}) and surface density (Σ_{tot}). The mass is calculated using

$$M_{\text{gas}} = 1.36 \times 1.1 \times 10^4 D_{\text{Mpc}}^2 S_{\text{CO}}, \quad (1)$$

where M_{gas} is in solar masses and S_{CO} is in Jy km s^{-1} .

The factor of 1.36 is the usual correction for elements other than hydrogen. This equation uses a CO-to- H_2 conversion factor of $2.8 \times 10^{20} \text{ cm}^{-2} (\text{K km s}^{-1})^{-1}$ (Bloemen et al. 1986). The exact value for the conversion factor is controversial and may vary by factors of 2–4 (see the discussion in Young & Scoville 1991). Σ is then calculated by dividing this gas mass by the area. Twelve of the 44 galaxies have relatively faint emission in the central kiloparsec; we list a 2σ upper limit for these galaxies. The results are shown in Tables 2 and 3 for the barred and unbarred spirals, respectively. Throughout this paper, we use the de Vaucouleurs et al. (1991, hereafter RC3) classification (SB and SAB) for barred spirals.

As noted earlier, we classify galaxies of type Sa–Sbc as early types and galaxies with types Sc–Sd as late types. Since a significant number of galaxies in SONG are type Sbc (14 of 44), we discuss briefly the motivation for the adopted division. It is based on the significant differences in the star formation properties between galaxies of type Sbc and earlier as opposed to those of later types (Ho et al. 1997). Since star formation depends on gas content, it is reasonable to use the same boundaries as Ho et al. (1997); otherwise comparison with previous studies becomes difficult. Furthermore, the division is also motivated by prior observational and theoretical work on properties of barred galaxies (Elmegreen & Elmegreen 1985; Combes & Elmegreen 1993; Huang et al. 1996). These studies have found a fundamental difference in the properties of early- and late-type bars. Early-type bars generally have a “flat” photometric profile, while late-type bars usually have an “exponential” profile. Of the 14 Sbc galaxies, 11 are barred spirals. We examined the optical/IR data for these 11 galaxies and find that 7 are clearly flat bars (NGC 2903, NGC 4321, NGC 4303, NGC 3992, NGC 3344, NGC 3953, and NGC 4051). The optical/IR data for the other four are not good enough to make a definitive classification, although the CO kinematics in NGC 5005 suggest that it too hosts a strong bar of the type usually found in early-type barred spirals. For these reasons, we place the Sbc galaxies in the early-type category.

In column (2) of Tables 2 and 3 we list the CO flux from the central kiloparsec in the combined (BIMA+NRAO 12 m single dish) maps for the 24 galaxies for which we collected on-the-fly (OTF) data. In column (3) we list the CO flux from the BIMA-only data. In most cases the BIMA-only data recover nearly all the CO flux. There are a few exceptions, in which the flux in the combined maps is 40%–50% higher than in the BIMA-only

⁶ The NRO-OVRO survey chose galaxies with integrated intensities of $I_{\text{CO}} > 10 \text{ K km s}^{-1}$ in any one of the $50''$ FCRAO pointings (typically the central pointing). We use the 10 K km s^{-1} selection as the division between CO-bright and CO-faint galaxies for the remainder of this paper.

⁷ The National Radio Astronomy Observatory is a facility of the NSF, operated under cooperative agreement by Associated Universities, Inc.

TABLE 1
BIMA SONG SAMPLE

Galaxy	α (J2000.0) ^a	δ (J2000.0) ^a	D_{25} ^b (arcmin)	P.A. ^c (deg)	i ^d (deg)	V_{Hel} ^e (km s ⁻¹)	D^f (Mpc)	Reference	Type (RC3)	OTF Data ^g
Barred										
NGC 0925	02 27 16.9	+33 34 44.0	10.5	102	55.8	553	9.3	1	SAB(s)d	...
IC 342	03 46 48.5	+68 05 46.0	21.4	37 ^h	31.0 ⁱ	34	2.1	2	SAB(rs)cd	Y
NGC 2403	07 36 51.3	+65 36 09.2	21.9	127	55.8	131	2.9	3	SAB(s)cd	...
NGC 2903	07 36 51.3	+65 36 09.2	12.6	17	61.4	556	7.3	4	SAB(rs)bc	Y
NGC 3184	10 18 16.9	+41 25 27.8	7.4	135	21.1	592	8.7	5	SAB(rs)cd	...
NGC 3344	10 43 31.1	+24 55 20.0	7.1	24	25.5	586	12.5	6	(R)SAB(r)bc	...
NGC 3351	10 43 57.7	+11 42 13.0	7.4	13	47.8	778	10.1	7	SB(r)b	Y
NGC 3368	10 46 45.7	+11 49 11.8	7.6	5	46.2	897	11.2	8	SAB(rs)ab	...
NGC 3521	11 05 48.5	-00 02 09.2	11	163	62.1	805	7.2	9	SAB(rs)bc	Y
NGC 3627	11 20 15.0	+12 59 28.6	9.1	173	62.8	727	11.1	10	SAB(s)b	Y
NGC 3726	11 33 21.1	+47 01 44.7	6.2	10	46.2	849	11.7	11	SAB(r)c	...
NGC 3953	11 53 49.0	+52 19 35.6	6.9	13	59.9	1054	14.1	12	SB(r)bc	...
NGC 3992	11 57 35.9	+53 22 28.3	7.6	68	51.9	1048	14.2	13	SB(rs)bc	...
NGC 4051	12 03 09.6	+44 31 52.5	5.3	135	42.2	725	9.4	14	SAB(rs)bc	...
NGC 4258	12 18 57.6	+47 18 13.4	18.6	150	67.1	448	7.3	15	SAB(s)bc	Y
NGC 4303	12 21 54.9	+04 28 24.9	6.5	7	27	1566	15.2	16	SAB(rs)bc	Y
NGC 4321	12 22 54.8	+15 49 20.6	7.4	30	31.7	1571	16.1	17	SAB(s)bc	Y
NGC 4490	12 30 36.3	+41 38 37.1	6.3	125	60.7	565	7.7	18	SB(s)d-pec	...
NGC 4535	12 34 20.3	+08 11 51.9	7.1	0	44.9	1961	16.0	19	SAB(s)c	...
NGC 4548	12 35 26.4	+14 29 46.8	5.4	150	37.4	486	15.9	20	SB(rs)b	...
NGC 4559	12 35 57.6	+27 57 35.1	10.7	150	66	815	9.7	21	SAB(rs)cd	...
NGC 4569	12 36 49.8	+13 09 46.3	9.6	23	62.8	-235	16.8	22	SAB(rs)ab	Y
NGC 4579	12 37 43.5	+11 49 05.1	5.9	95	37.4	1519	16.8	23	SAB(rs)b	...
NGC 4699	12 49 02.18	-08 39 51.4	3.8	45	46.2	1427	19.0	24	SAB(rs)b	...
NGC 4725	12 50 26.6	+25 30 02.7	10.7	35	44.9	1206	12.6	25	SAB(r)ab-pec	...
NGC 5005	12 50 26.6	+25 30 02.7	5.8	65	61.4	946	21.3	26	SAB(rs)bc	Y
NGC 5248	13 37 32.0	+08 53 06.2	6.2	110	43.6	1153	22.7	27	SAB(rs)bc	Y
NGC 5457	14 03 12.5	+54 20 55.5	28.8	35	21.1	241	6.5	28	SAB(rs)cd	Y
NGC 6946	20 34 52.3	+60 09 13.2	11.5	35	31.7	48	6.4	29	SAB(rs)cd	Y
Unbarred										
NGC 0628	01 36 41.7	+15 47 00.5	10.5	25	24.2	657	7.3	30	SA(s)c	Y
NGC 1068	02 42 40.7	-00 00 47.8	7.1	70	31.7	1136	18.0	31	(R)SA(rs)b	Y
NGC 2841	09 22 02.6	+50 58 35.3	8.1	147	64.1	638	9.5	32	SA(r)b	...
NGC 2976	09 47 15.4	+67 54 59.0	5.9	143	62.8	3	4.3	33	SAC-pec	...
NGC 3031	09 55 33.1	+69 03 54.9	26.9	157	58.4	-34	3.3	34	SA(s)ab	...
NGC 3938	11 52 49.4	+44 07 14.6	5.4	20	14	809	11.3	35	SA(s)c	Y
NGC 4414	12 26 27.08	+31 13 24.7	3.6	155	55.8	716	19.1	36	SA(rs)c?	Y
NGC 4450	12 28 29.6	+17 05 05.8	5.3	175	42.2	1954	16.0	37	SA(s)ab	...
NGC 4736	12 50 53.1	+41 07 12.5	11.2	105	35.6	308	6.6	38	(R)SA(r)ab	Y
NGC 4826	12 56 43.6	+21 40 57.6	10	115	57.5	408	5.0	39	(R)SA(rs)ab	Y
NGC 5033	13 13 27.5	+36 35 37.1	10.7	170	62.1	875	21.3	40	SA(s)c	Y
NGC 5055	13 15 49.3	+42 01 45.4	12.6	105	54.9	504	7.2	41	SA(rs)bc	Y
NGC 5194	13 29 52.6	+47 11 42.9	11.2	163	51.9	463	8.4	42	SA(s)bc-pec	Y
NGC 5247	13 38 03.0	-17 53 02.5	5.6	20	29.4	1357	15.2	43	SA(s)bc	Y
NGC 7331	22 37 04.0	+34 24 57.3	10.5	171	69.2	821	15.1	44	SA(s)b	Y

NOTE.—Units of right ascension are hours, minutes, and seconds, and units of declination are degrees, arcminutes, and arcseconds.

^a 2MASS Galaxy Centers from the LGA (Jarrett et al. 2003).

^b Optical diameter (RC3).

^c Position angle (RC3).

^d Inclination (RC3).

^e Heliocentric velocity (NASA/IPAC Extragalactic Database).

^f Adopted distance; reference given in column to the right.

^g Indicates whether on-the-fly data were collected as part of SONG.

^h Galaxies in common between SONG and NRO-OVRO sample (Sakamoto et al. 1999b).

ⁱ From kinematic fitting, Crothwaite et al. (2000).

REFERENCES.—(1) Sohn & Davidge 1998; (2) Karachentsev & Tikhonov 1993; (3) Metcalfe & Shanks 1991; (4) Planesas et al. 1997; (5) Pompei & Natali 1997; (6) Corbelli et al. 1989; (7) Graham et al. 1997; (8) Tanvir et al. 1999; (9) Thornley 1996; (10) Saha et al. 1999; (11) van der Kruit 1971; (12) RC3, using $H_0 = 75$; (13) Gottesman & Hunter 1982; (14) Liszt & Dickey 1995; (15) Herrnstein et al. 1997; (16) Molla et al. 1999; (17) Ferrarese et al. 1996; (18) Tully 1988; (19) Macri et al. 1999; (20) Graham et al. 1999; (21) Vogler et al. 1996; (22) Barth et al. 1998; (23) Ho 1999a; (24) Bower et al. 1993; (25) Gibson et al. 1999; (26) Barth et al. 1998; (27) Tully 1988; (28) Stetson et al. 1998; (29) Sharina et al. 1997; (30) Sharina et al. 1996; (31) literature values vary from 14 to 22 Mpc; 18 Mpc is assumed as midpoint value; (32) Block et al. 1999; (33) Karachentsev et al. 1991; (34) Paturel et al. 1998; (35) Jiménez-Vicente et al. 1999; (36) Turner et al. 1998; (37) Tully 1988; (38) Mulder & Driel 1993; (39) Rubin 1994; (40) Ho et al. 1999b; (41) Tully 1988; (42) Feldmeir et al. 1997; (43) Grosbol & Patsis 1998; (44) Hughes et al. 1998.

TABLE 2
DERIVED PROPERTIES FOR BARRED SONG GALAXIES

Galaxy (1)	$S_{\text{nuc}}^{\text{CO}}$ COMB ^a (Jy km s ⁻¹) (2)	$S_{\text{nuc}}^{\text{CO}}$ BIMA ^a (Jy km s ⁻¹) (3)	rms in BIMA (Jy km s ⁻¹) (4)	$M_{\text{nuc}}^{\text{b}}$ (10 ⁷ M_{\odot}) (5)	$\Sigma_{\text{nuc}}^{\text{c}}$ (M_{\odot} pc ⁻²) (6)	$S_{\text{tot}}^{\text{COd}}$ (Jy km s ⁻¹) (7)	$M_{\text{tot}}^{\text{e}}$ (10 ⁸ M_{\odot}) (8)	$\Sigma_{\text{tot}}^{\text{f}}$ (M_{\odot} pc ⁻²) (9)	$\Sigma_{\text{nuc}}/\Sigma_{\text{tot}}^{\text{g}}$ (10)
Early Types									
NGC 2903.....	462	447	13	35.6	454	2740	22.0	3.89	117
NGC 3344 ^h	2	8	3.70 ^h	47.6 ^h	520	12.0	2.30	20.7 ^h
NGC 3351.....	207	208	9	31.7	404	700	10.7	2.88	140
NGC 3368.....	...	309	11	58.0	738	610	11.5	2.38	310
NGC 3521 ^h	53	4	15	2.30 ^h	30.0 ^h	4920	38.2	9.15	3.28 ^h
NGC 3627.....	244	233	7	43.0	546	4660	85.8	12.7	43.1
NGC 3953 ^h	7	9	5.40 ^h	68.0 ^h	1790	53.2	8.90	8.04 ^h
NGC 3992 ^h	6	8	4.80 ^h	62.0 ^h	...	7.00 ⁱ	2.00 ⁱ	31.0 ⁱ
NGC 4051.....	...	103	3	13.6	173	740	9.80	5.93	29.2
NGC 4258.....	180	176	13	14.0	179	1240	9.90	0.81	221
NGC 4303.....	135	122	4	42.0	537	2280	78.8	12.2	44.0
NGC 4321.....	140	132	5	51.0	651	3340	129	13.7	47.5
NGC 4548.....	...	26	5	9.80	125	540	20.4	4.20	29.8
NGC 4569.....	141	136	5	57.0	731	1500	63.0	3.66	200
NGC 4579.....	...	43	8	18.2	231	910	38.0	5.88	39.3
NGC 4699 ^h	3	6	6.50 ^h	83.0 ^h
NGC 4725 ^h	15	16	7.60 ^h	97.0 ^h	1950	46.0	3.83	25.3 ^h
NGC 5005.....	...	80	2	54.0	691	1260	85.0	8.40	82.3
NGC 5248.....	57	54	2	42.0	515	1190	92.0	6.97	76.0
Late Types									
IC 342.....	2379	1713	75	11.3	144	29220	19.0	14.4	10.0
NGC 0925 ^h	6	10	2.60 ^h	33.0 ^h	960	12.0	1.96	16.8 ^h
NGC 2403 ^h	15	19	0.50 ^h	6.10 ^h	540	0.70	0.25	24.4 ^h
NGC 3184.....	...	60	7	6.80	87.0	1120	13.0	4.60	18.9
NGC 3726.....	...	33	3	6.80	86.0	720	14.7	4.22	20.4
NGC 4490 ^h	0	3	0.50 ^h	6.80 ^h	480	4.00	2.70	2.52 ^h
NGC 4535.....	...	110	5	42.0	536	1570	60.0	7.00	76.6
NGC 4559.....	...	21	9	2.96	38.0	...	4.00 ⁱ	0.50 ⁱ	76.0 ⁱ
NGC 5457.....	123	116	7	7.30	93.0	...	14.9 ⁱ	4.90 ⁱ	19.0
NGC 6946.....	1691	1747	15	107	1363	12370	76.0	21.1	64.7

^a CO flux in central kiloparsec measured from BIMA SONG.

^b Total gas mass in the central kiloparsec calculated from the SONG flux. All masses are calculated using $M = 1.36 M(\text{H}_2)$, $M(\text{H}_2) = 1.1 \times 10^4 D^2 S_{\text{CO}}$, where D is in Mpc and S_{CO} is in Jy km s⁻¹. We use a CO to H₂ conversion factor of 2.8×10^{20} cm⁻² (K km s⁻¹)⁻¹, 7% smaller than Sakamoto et al. (1999b).

^c Nuclear gas surface density derived by dividing the mass by $\pi(500 \text{ pc})^2$.

^d Total CO flux from galaxy (disk+nucleus) from the FCRAO survey (Young et al. 1995).

^e Total gas mass in the galaxy (disk+nucleus) calculated from the FCRAO flux.

^f Total gas surface density in the galaxy (disk+nucleus) calculated from the FCRAO flux.

^g Ratio of the nuclear gas surface density to the disk gas surface density, defined as f_{con} in § 1.

^h 2 σ upper limit.

ⁱ Using galaxy-averaged flux from SONG data instead of the FCRAO survey.

maps: IC342, NGC 0628, NGC 3521, and NGC 4414. In these cases, the relative angular sizes of the beam and galaxy, the inclination, or the CO distribution likely have contributed to spatial filtering or beam-smearing effects.

We choose to use the BIMA-only maps to measure M_{nuc} because in most cases the BIMA-only fluxes are consistent with M_{nuc} from the combined map (see also Fig. 53 in Helfer et al. 2003 and the discussion in Helfer et al. 2002). There is no evidence that barred or unbarred spirals are preferentially affected by the lack of single-dish data, and we want to use as homogeneous a data set as possible. We did not correct the BIMA-only data for beam smearing. Our typical 6'' beam subtends an area of diameter of <1 kpc for almost all galaxies in our sample, as can be seen in Table 2 in Helfer et al. (2003), where the area subtended is shown in the plane of the sky. In the plane of a galaxy, the beam may subtend a larger region (at most by $\cos i^{-1}$) along the galaxy minor axis. For the galaxies in our sample this cor-

rection is less than a factor of 2 ($i < 60^\circ$), and therefore our beam typically subtends <1 kpc along the minor axis of the galaxy plane.

In our analysis we also plot the seven additional galaxies from the NRO-OVRO survey that are not in common with SONG; these include five unbarred galaxies, which are rarer in both samples. We confirm that the SONG data are consistent with the NRO-OVRO data by comparing the measured fluxes for the 13 galaxies in common between the two samples; after accounting for differences in the CO-to-H₂ conversion factor and adopted distances, the fluxes are consistent within the errors.

We derive M_{tot} from the global CO fluxes obtained by the FCRAO survey (Table 3 in Young et al. 1995); these fluxes were derived from fitting an exponential CO profile to several discrete pointings along the major and minor axis of each galaxy. SONG, on the other hand, measured the CO fluxes using OTF maps for 24 galaxies and discrete pointings for the remaining

TABLE 3
DERIVED PROPERTIES FOR UNBARRED SONG GALAXIES

Galaxy (1)	$S_{\text{nuc}}^{\text{CO}}$ COMB ^a (2)	$S_{\text{nuc}}^{\text{CO}}$ BIMA ^a (Jy km s ⁻¹) (3)	rms in BIMA (4)	$M_{\text{nuc}}^{\text{b}}$ ($10^7 M_{\odot}$) (5)	$\Sigma_{\text{nuc}}^{\text{c}}$ ($M_{\odot} \text{ pc}^{-2}$) (6)	$S_{\text{tot}}^{\text{COd}}$ (Jy km s ⁻¹) (7)	$M_{\text{tot}}^{\text{e}}$ ($10^8 M_{\odot}$) (8)	$\Sigma_{\text{tot}}^{\text{f}}$ ($M_{\odot} \text{ pc}^{-2}$) (9)	$\Sigma_{\text{nuc}}/\Sigma_{\text{tot}}^{\text{g}}$ (10)
Early Types									
NGC 1068.....	120	116	9	56.0	716	5160	250	23.0	31.1
NGC 2841 ^h	-11	14	3.80 ^h	48.0 ^h	1870	25.0	6.40	7.50 ^h
NGC 3031.....	...	37	34	1.10 ^h	14.0 ^h	...	10.0 ⁱ	1.00 ⁱ	14.0 ⁱ
NGC 4450.....	...	12	5	3.80	49.0	450	17.0	3.60	13.6
NGC 4736.....	239	190	15	12.4	157	2560	17.0	4.60	34.1
NGC 4826.....	760	769	24	28.8	366	2170	8.10	4.90	74.7
NGC 5055.....	302	267	13	20.7	264	5670	44.0	8.00	33.0
NGC 5194.....	103	81	11	8.55	109	9210	97.0	16.5	6.61
NGC 5247.....	29	20	3	6.90	88.0	1030	36.0	7.40	11.9
NGC 7331 ^h	4	-3	8	5.50 ^h	69.0 ^h	4160	142	8.50	8.12 ^h
Late Types									
NGC 0628.....	41	26	8	2.10	26.0	2160	17.0	4.40	5.91
NGC 2976.....	...	21	5	0.58	7.40	610	1.70	3.90	1.90
NGC 3938.....	38	30	6	5.70	73.0	1750	33.0	13.5	5.41
NGC 4414.....	10	4	2	2.20	28.0	2740	150	47.0	0.60
NGC 5033.....	35	34	6	23.0	294	1640	111	3.20	91.9

^a CO flux in central kiloparsec measured from BIMA SONG.

^b Total gas mass in the central kiloparsec calculated from the SONG flux. All masses are calculated using $M = 1.36M(\text{H}_2)$, $M(\text{H}_2) = 1.1 \times 10^4 D^2 S_{\text{CO}}$, where D is in Mpc and S_{CO} is in Jy km s⁻¹. We use a CO to H₂ conversion factor of $2.8 \times 10^{20} \text{ cm}^{-2} (\text{K km s}^{-1})^{-1}$, 7% smaller than Sakamoto et al. (1999b).

^c Nuclear gas surface density derived by dividing the mass by $\pi(500 \text{ pc})^2$.

^d Total CO flux from galaxy (disk+nucleus) from the FCRAO survey (Young et al. 1995).

^e Total gas mass in the galaxy (disk+nucleus) calculated from the FCRAO flux.

^f Total gas surface density in the galaxy (disk+nucleus) calculated from the FCRAO flux.

^g Ratio of the nuclear gas surface density to the disk gas surface density, defined as f_{con} in § 1.

^h 2 σ upper limits.

ⁱ Using galaxy-averaged flux from SONG data instead of the FCRAO survey.

galaxies. The SONG fluxes are consistent with the FCRAO survey (see Fig. 51 in Helfer et al. 2003). In the five cases for which we did not have FCRAO fluxes, we used the SONG fluxes for M_{tot} where available. These are also listed in Tables 2 and 3.

We measured M_{nuc} in the central kiloparsec because, as discussed in § 1, most of the evolutionary effects depend on the accumulation of gas near the nucleus. The choice is also partially influenced by Sakamoto et al. (1999a, 1999b), who showed that more than half of the galaxies in their sample have nuclear concentrations that are well described by an exponential scale length of less than 500 pc. Though galaxies in the SONG data set are less strongly concentrated (many are not even centrally peaked; see Regan et al. 2001), examining the inner kiloparsec provides consistency with the previous study. A different measure of nuclear gas properties might be a dynamical length scale such as the radius of the largest stable x_2 orbit. However, locating the largest stable x_2 orbit requires precise measurements of the rotation curve and potential (Regan & Teuben 2003). This is difficult near the nuclei of galaxies due to the lack of high-resolution data and the presence of streaming motions induced by the bar. Another measure might be to choose a bulge radius as determined from near-infrared images, but deriving a unique bulge-disk decomposition is difficult. Yet another measure might be to choose a distance that is a standard fraction of the galaxy diameter. This choice is problematic because there is no evidence that nuclear properties of galaxies are connected with the disk properties. In fact, star formation properties of the circum-nuclear regions are known to be distinct from those of the disk

(Kennicutt 1998). Hence, we choose the central kiloparsec as our fiducial diameter for the nuclear region.

3. RESULTS

3.1. Molecular Gas Masses in the Central Kiloparsec of Barred and Unbarred Galaxies

The mass of the molecular gas in the central kiloparsec (M_{nuc}) is plotted in Figure 1 against the total molecular gas mass in the galaxy (M_{tot}).⁸ Barred spirals are shown with a circle and unbarred spirals with a triangle. SONG galaxies have filled symbols. The data from Sakamoto et al. (1999b) for galaxies not in common with the SONG sample are marked with open symbols. The diagonal lines indicate the fraction of the total gas mass in the central kiloparsec.

Before we discuss the nuclear masses, we note that there is no obvious difference in the distribution of M_{tot} between barred and unbarred spirals. The range for M_{tot} spans $\sim 10^8 - 10^{10} M_{\odot}$. For the entire SONG sample, the mean total molecular gas mass is $\langle M_{\text{tot}} \rangle_{\text{bar}} = (4 \pm 1) \times 10^9 M_{\odot}$ for the barred spirals and $\langle M_{\text{tot}} \rangle_{\text{unbar}} = (6 \pm 2) \times 10^9 M_{\odot}$ for the unbarred spirals. If we compare the red symbols (early types) to the blue symbols (late types), there is also no obvious difference in M_{tot} -values between early and late Hubble-type galaxies. This is consistent with

⁸ NGC 4699 is not shown in any of the figures because it only has an upper limit for the single-dish flux. However, it is one of the galaxies with an upper limit for M_{nuc} and has no gas in its bar.

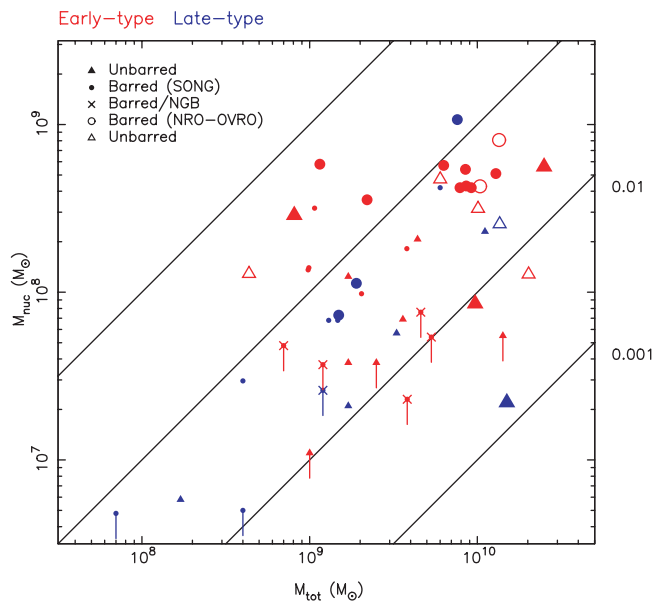


FIG. 1.—Plot of molecular gas mass in solar masses in the central kiloparsec (y -axis) and integrated over the entire galactic disk (x -axis). The diagonal lines indicate the molecular gas mass fraction in the central kiloparsec. The barred spirals are represented with circles, and the unbarred spirals with triangles. Solid symbols are SONG data, whereas open symbols are data from galaxies not in common with SONG from Sakamoto et al. (1999b). The crosses mark galaxies that have no gas in the bars (NGB). Galaxies with only upper limits are shown with a small vertical segment. Larger symbols reflect galaxies that are **CO**-bright ($I_{\text{CO}} > 10 \text{ K km s}^{-1}$ in an FCRAO pointing).

large single-dish surveys of molecular gas in galaxies (e.g., Sage 1993; Young et al. 1995).

The fraction of the molecular gas that is in the central kiloparsec varies by almost 3 orders of magnitude, from 0.001 to nearly 0.6. Figure 1 shows that galaxies with the highest values of this fraction and also those with the highest M_{nuc} are mainly early types, especially bars. Of the eight galaxies with nuclear gas mass fractions above 0.1, six are barred, and five of these six are early Hubble-type galaxies.

Another eight barred spirals have only upper limits for their nuclear molecular gas mass. Five of these are early-type bars; not only is no gas detected in the central kiloparsec, but none is detected within the entire region interior to the bar. The existence of early-type barred spirals without any nuclear gas is consistent with bar-driven gas transport, as we discuss in the next section. In addition, we note that these results contrast with the emphasis of previous studies on large excesses of molecular gas in the central kiloparsec (Sakamoto et al. 1999b; Jogee et al. 2005). For example, Jogee et al. (2005) conclude that the central kiloparsec of barred spirals is significantly different from the outer disks with molecular gas masses in excess of $2 \times 10^8 M_{\odot}$ up to $3 \times 10^9 M_{\odot}$. However, for the barred spirals in SONG, we find a range of nuclear masses from 10^7 to $10^9 M_{\odot}$, with a mean of $\sim 2 \times 10^8 M_{\odot}$. Indeed, 18 of 29 barred spirals in SONG have $M_{\text{nuc}} < 2 \times 10^8 M_{\odot}$. Clearly the high M_{nuc} -values emphasized by previous studies apply only to a subset of barred galaxies.

3.2. Bar-driven Gas Transport

In Figure 2 we plot the molecular gas surface density for the central kiloparsec (Σ_{nuc}) versus that averaged over the galaxy disk inside D_{25} (Σ_{tot}) for all galaxies shown in Figure 1. The diagonal lines now indicate constant values of the central concentration parameter, f_{con} , which we discussed in § 1.

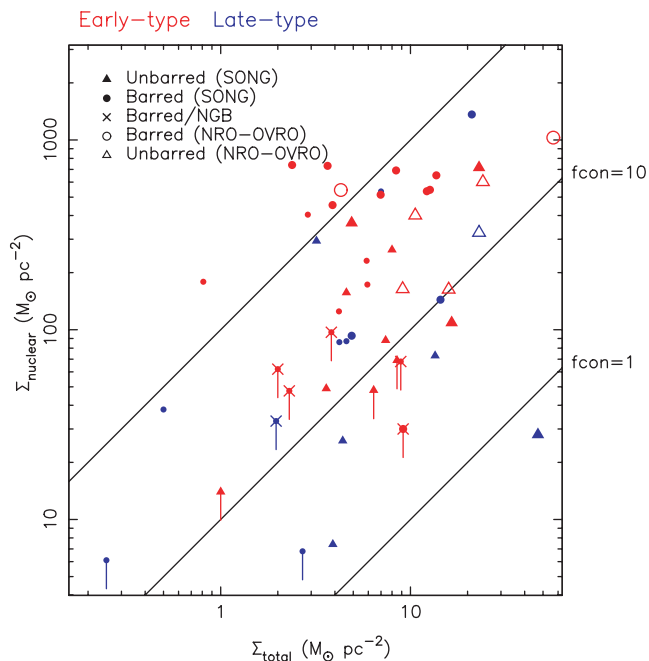


FIG. 2.—Same as Fig. 1, but with the axes now reflecting the molecular gas surface densities in solar masses per square parsec. The diagonal lines show the concentration index defined as the ratio of the nuclear molecular gas surface density to the total molecular gas surface density.

The figure immediately shows a clear difference in central concentration (f_{con}) between barred and unbarred spirals. All six galaxies with $f_{\text{con}} > 100$ are barred spirals. At the other end, for $f_{\text{con}} < 10$, 7 of the 10 galaxies are unbarred. The higher f_{con} -values in barred spirals thus provide the strongest and most direct evidence for bar-driven gas transport, consistent with the results of Sakamoto et al. (1999b).

3.2.1. Bar Gas Transport in **CO**-faint Galaxies

As most of the highest f_{con} -values are in **CO**-bright galaxies (*larger symbols*), we specifically address the question of whether bars also enhance f_{con} in **CO**-faint galaxies. Figure 3 shows only the 26 (16 barred and 10 unbarred) SONG galaxies with FCRAO brightnesses $< 10 \text{ K km s}^{-1}$. We see that for $f_{\text{con}} > 10$, 9 of the 13 galaxies with significant detections in both total and nuclear surface densities are barred. Dividing the 26 **CO**-faint galaxies into two bins, we see that 11 of the 13 highest f_{con} galaxies are barred, compared with only 5 of the lowest 13 f_{con} galaxies. Thus, even in the sample of galaxies that are not **CO**-bright, we conclude that there is evidence for bar-induced gas transport. This evidence is further strengthened upon noting that most of the low- f_{con} barred galaxies have no gas at all within the bar corotation radius. The corotation radius is believed to be at 1.2 times bar end (e.g., Athanassoula 1992b). Galaxies without gas in the bar region can be understood as those in which bar-driven accretion has proceeded to the point at which all the gas presently available to the bar has already been driven to the central region and converted into stars.

Jogee et al. (2005), in a paper that focused on the role of bars in starbursts and secular evolution, proposed an evolutionary sequence for bars and starbursts. In type I nonstarbursts, gas is still distributed through the bar region and is only beginning to accumulate in the central region. Type II nonstarbursts have significant central concentrations, but the gas has yet to accumulate to the surface densities required for a starburst. In starbursts, the sufficient gas has accumulated to drive a starburst.

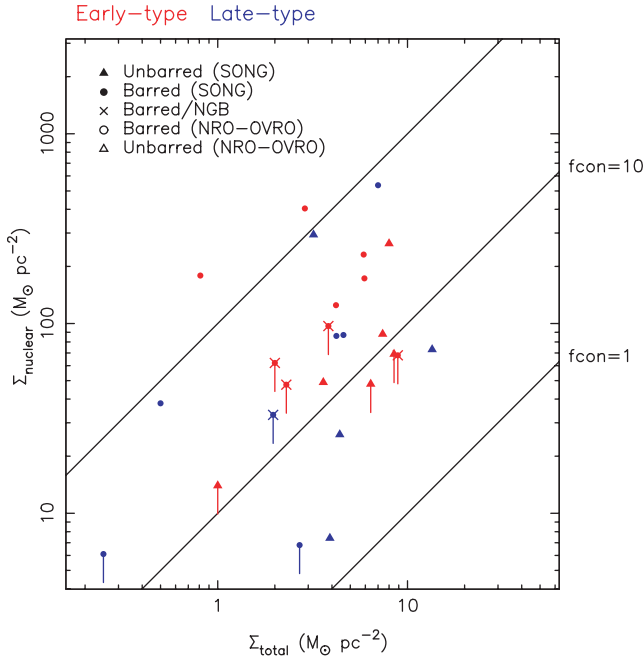


Fig. 3.—Same as Fig. 2, but showing only the CO-faint galaxies.

We would therefore add a category, type III nonstarbursts, which are galaxies in the poststarburst phase. All the gas within the radius swept by the bar has already been driven to the nucleus and has been consumed by a starburst (or sufficient gas has been consumed so that the current gas surface density is lower than the critical density needed for a starburst). It would be interesting to look for evidence of this in the stellar populations. Such galaxies will be free of molecular gas within the bar region until some event enables the feeding of gas through the barrier that seems to be present near the bar corotation radius. If this happens, then central gas accumulations and starbursts would be episodic.

3.2.2. Bar Gas Transport as a Function of Hubble Type

First we consider early Hubble-type barred spirals, which we take to be Hubble types Sbc and earlier. There are 26 early-type galaxies in SONG, plus 6 from the Sakamoto sample; these are shown in Figure 4. For galaxies above the median f_{con} for early-type galaxies, 13 of 16 are barred, compared with only 7 of 16 below the median. The median f_{con} for the early-type bars is 43, compared with 14 for the unbarred early types. Clearly, the evidence for bar driven inflow in early-type galaxies is very strong.

Next we consider the 16 late-type spirals, shown in Figure 5. For galaxies above the median f_{con} , seven of eight are barred spirals, whereas for galaxies below the median, only three of eight are barred. The median f_{con} for late-type bars is 20, 3 times higher than that for unbarred late-type galaxies. Thus there is also good evidence for inflow in late-type bars. We conclude that bars transport gas inward regardless of Hubble type.

Although both early- and late-type bars have f_{con} -values about 3 times higher than their unbarred counterparts, note that the median f_{con} for early-type barred galaxies is about twice that for late-type bars. Also, the median Σ_{nuc} ($M_{\odot} \text{pc}^{-2}$) for barred early types is 400, compared to 87 for late-type bars. In part, the higher f_{con} and Σ_{nuc} for early types can be understood as a consequence of the higher critical surface density threshold for star formation in early types resulting from their steeper rotation curves. This is probably the reason why even among the unbarred spirals in our sample, the early-type galaxies have about

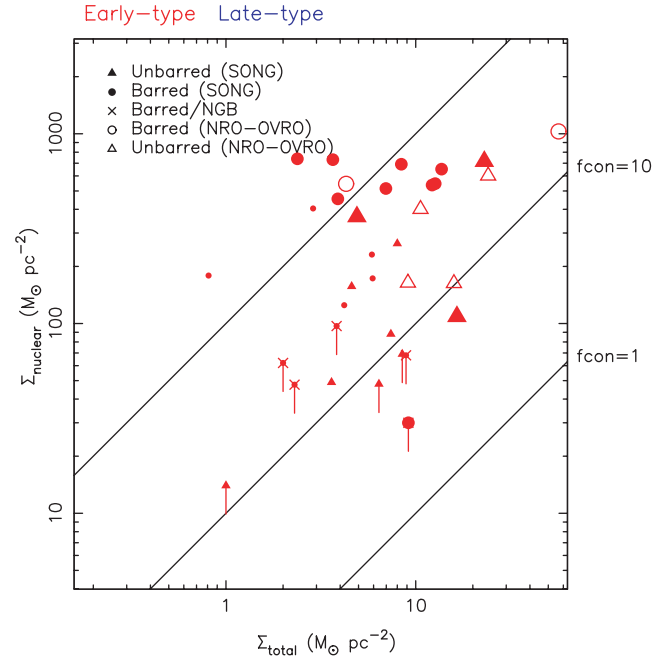


Fig. 4.—Same as Fig. 2, but showing only the early Hubble-type (Sa–Sbc) galaxies are shown.

a 3 times higher median f_{con} and Σ_{nuc} compared to those for the late types; however, this comparison should be viewed with caution because of the small number of unbarred galaxies.

Ho et al. (1997) attributed the higher star formation rates in early-type bars to the higher critical density threshold and predicted the higher gas surface densities that we indeed find. However, for early-type bars to *maintain* these higher central mass concentrations requires that the early-type bars have significantly higher mass inflow rates than late-type bars. This is because the gas consumption rate implied by the star formation rates observed

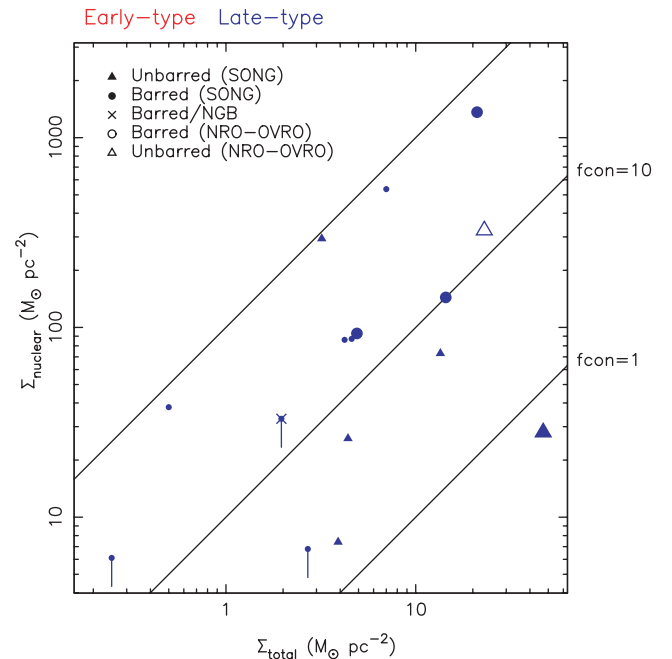


Fig. 5.—Same as Fig. 2, but showing only the late Hubble-type (Sc–Sdm) galaxies.

by Ho et al. are higher in early types—the median value of the star formation rate in barred early types is $0.08 M_{\odot} \text{ yr}^{-1}$, compared to $0.007 M_{\odot} \text{ yr}^{-1}$ in barred late types. That is, not only are the median surface densities and nuclear masses a factor of 4 higher in early-type bars, but the gas is consumed at a typical rate more than 10 times higher. Clearly, the mass inflow rates in early types must be much higher than for late-type bars.

How can we explain this difference? We believe the reason is related to the different type of bars that are typically found in early and late Hubble-type galaxies: “flat” and “exponential” (Elmegreen & Elmegreen 1985, 1996; Ohta et al. 1986; Combes & Elmegreen 1993). Flat bars, found primarily in early-type galaxies, have a rectangular appearance with flat shoulders in their photometric profile, are usually associated with grand-design spiral structure, and lie in the flat part of the rotation curve. They are also longer relative to their disks and have higher amplitudes. Exponential bars, on the other hand, are located in the rising part of a rotation curve, and are oval, rather than rectangular in appearance. Their photometric profile is exponential, similar to a galactic disk. They are shorter relative to their disks than flat bars and have a lower amplitude. Exponential bars are primarily found in late Hubble-type spirals.

Bars in early-type galaxies, i.e., flat bars, are predicted to be more effective at driving gas inward, because longer bars encounter more gas in the disk and because the higher nonaxisymmetry leads to a higher inflow rate. N -body (Combes & Elmegreen 1993) and hydrodynamic models (Regan & Teuben 2004) predict that weaker bars (fatter bars and/or less massive bars) drive significantly less mass inward. The evidence presented here thus supports the predictions of higher inflow rates in early-type barred spirals.

Another possibility is that the higher CO fluxes in the nuclei of early-type galaxies may reflect a change in the CO emissivity due to higher pressures and velocity dispersions in the bulge region (see the discussion in Regan et al. 2001). The increased star formation in the nuclei of early-type spirals may also contribute to an increase in the pressure. But if there is indeed less gas at the centers of early types, then the enhanced star formation implies a higher efficiency and decreased gas consumption times. Then the presence of a large fraction of early-type bars with high central concentration of CO emission is surprising. A quantitative discussion of this awaits better extinction-corrected star formation rates.

3.3. Secular Evolution From Late- to Early-Type Galaxies?

Several studies have suggested that galaxies undergo secular evolution via bar-driven inflows. One popular evolutionary scenario is the change of late-type galaxies into early types via bar inflows (Friedli & Benz 1995; Zhang 1999). We argue that such a transformation is unlikely. In order for a late-type galaxy to build an early-type bulge, it would need to add $\sim 10^{10}$ to $\sim 10^{11} M_{\odot}$ of gas that must then be converted to stars (Binney & Merrifield 1998). If we take the best-case scenario for such a transformation, i.e., assume that bars (1) are long lived (10 Gyr), (2) transport gas inward at sufficiently high rates, (3) have an adequate supply of molecular gas, (4) convert enough of the accumulated gas to stars, and (5) scatter the stars in the vertical dimension to build a bulge, then a late-type galaxy can build an early-type bulge. Some of these conditions are difficult, if not impossible, to reconcile with observational data.

While the high bar fraction at $z > 0.7$ (Sheth et al. 2003) suggests that bars are likely to be long lived, it is unlikely that the mass inflow rates or the gas reservoir in late Hubble-type galaxies are sufficient to build an early-type bulge. Based on the

differences in f_{con} -values, we noted that the mass inflow rate in late Hubble-type galaxies is lower than in early Hubble types. The inflow rate in the NRO-OVRO sample was estimated by Sakamoto et al. (1999b) to be $\sim 0.1\text{--}1 M_{\odot} \text{ yr}^{-1}$. In later type galaxies the rate would be even lower. We note that at the median nuclear star formation rate for late-type bars measured by Ho et al. (1997) data ($0.007 M_{\odot} \text{ yr}^{-1}$), it would take 10^{12} yr to build even a $10^{10} M_{\odot}$ bulge. At the upper end of gas consumption rates for late-type bars ($1 M_{\odot} \text{ yr}^{-1}$), it would be possible to build a small bulge in 10^{10} yr; however, the data demonstrate that this is certainly not typical.

Moreover, late-type bars are small and do not have access to a vast molecular gas reservoir. In SONG, the average length of a late-type bars is 3 kpc (the average length of bars in the entire sample is 5 kpc; Sheth 2001). To measure the available gas reservoir, let us assume this length and the average Σ_{tot} for SONG ($8 M_{\odot} \text{ pc}^{-2}$). Then the available gas reservoir for a typical late-type spiral is only $5 \times 10^7 M_{\odot}$. This value may be higher because the average Σ_{tot} is a measurement over the entire disk. In the bar region, the available gas reservoir may be higher. But even if we assume a Σ that is 10 times higher, i.e., $80 M_{\odot} \text{ pc}^{-2}$, the gas reservoir would still be too small. It is possible that accretion from mergers or gas transport from outer parts of the galactic disk may increase this number but it is at least 2 orders of magnitude lower than that required for creating an early-type bulge in a late-type galaxy. Thus, we believe that it is unlikely that a late-type galaxy evolves into an early type, consistent with Kormendy & Kennicutt (2004).

This, however, does not imply that there is no secular evolution in barred spiral galaxies. To the contrary, the evidence presented here for bar-driven gas inflows, combined with the enhanced star formation activity in barred spirals, indicates that the central regions of barred galaxies undergo significant changes. They are probably the most important changes in the evolution of disks, since $z \sim 1$ when the merging activity began to decline (Baugh et al. 1996; Ferguson et al. 2000). Another possible secular evolutionary sequence could be the dissolution of bars by an increasing central concentration of mass. Models have been used to debate the exact impact of increasing central concentration (e.g., Friedli & Benz 1993; Norman et al. 1996; Bournaud & Combes 2002; Athanassoula 2003; Shen & Sellwood 2004). Tentative evidence for such dissolution was presented in Das et al. (2003), who showed a correlation between the bar ellipticity and the central mass concentration.

The data presented here lend credence to the formation of pseudobulges in barred spirals; pseudobulges and secular evolution via gas inflows have recently been reviewed by Kormendy & Kennicutt (2004). In this context, we particularly point out the significant population of early-type barred spirals (6 of 19) that have no molecular gas detected in nuclear region and very little detected in the region within the bar corotation radius. This suggests that the gas inside the bar corotation radius has already been driven into the nuclear region, where it has been consumed by star formation. Among the late-type spirals, there are three barred galaxies with upper limits to the molecular gas in the central kiloparsec. One of them has no gas within the bar corotation radius. As already discussed, the process of gas accretion is slower in late types. The star formation rates in late types are also lower, because late-type spirals have lower Σ_{crit} , the critical gas surface densities for star formation (e.g., Toomre 1964; Kennicutt 1989). So it is not unusual to find fewer examples of late-type barred spirals with no gas in the center and bar regions. The secular evolutionary sequence of gas inflow and subsequent star formation simply occurs at a slower pace in these galaxies;

over time, even the late-type spirals will build pseudobulges. Signatures of poststarburst populations in barred spirals with low M_{nuc} and little gas in the bar region would provide further confirmation of this evolutionary sequence.

Another way to interpret the galaxies without gas in the center is that a third of the barred galaxies, whether they are early type or late type, are in a quiescent state, i.e., without measurable gas in the center or the bar region. This indicates that if the fueling via bars is periodic, then bars are “actively” fueling the center two-thirds of the time. When better measurements of gas inflow are obtained, this duty cycle will need to be taken into account to measure the impact of the gas inflow over the lifetime of the bar and galaxy.

4. CONCLUSIONS

With a larger and more representative sample of nearby galaxies from SONG, we compared the central concentration of molecular gas in both CO-bright and CO-faint spiral galaxies spanning a range of Hubble types. In all cases we found clear evidence of more centrally concentrated molecular gas distributions in barred spirals. This is the strongest and most conclusive evidence for the bar-driven transport of molecular gas to the central kiloparsec of galaxies.

We find that barred spirals of late Hubble types are less centrally concentrated than early Hubble types. This, coupled with the enhanced star formation activity observed in early-type bars, indicates higher mass accretion rates in early Hubble-type spirals. The differences are probably related to the longer and

stronger “flat” bars that are found preferentially in early Hubble-type galaxies. The observation of a significant subset of early-type barred spirals with little or no gas within the bar region is consistent with higher accretion rates; these galaxies have the expected conditions of a poststarburst galaxy, where the large stockpiles of gas driven inward by the bar have already been converted into stars.

Contrary to previous suggestions, the evidence indicates that it is highly unlikely for a late-type galaxy to evolve into an early type via bar-induced gas inflow. Nonetheless, secular evolutionary processes are undoubtedly present, and pseudobulges are inevitable because of the bar-induced gas inflow. Evidence for pseudobulges is likely to be clearest in early-type galaxies because of their higher inflow rates and higher star formation activity.

The authors are indebted to the referee for the detailed and thorough examination of this manuscript and the many helpful comments and suggestions that s/he provided. This work would not have been possible without the rest of the SONG team members (T. Helfer, T. Wong, L. Blitz, and D. Bock) and the dedicated observatory staff at Hat Creek and at the Laboratory for Millimeter-Wave Astronomy at the University of Maryland. We thank T. Beasley, D. M. Elmegreen, B. G. Elmegreen, A. Harris, J. Kenney, J. Knapen, N. Scoville, E. Schinnerer, I. Shlosman, L. E. Strubbe, and T. Treu for invaluable and insightful discussions.

REFERENCES

- Athanassoula, E. 1992a, *MNRAS*, 259, 328
 ———. 1992b, *MNRAS*, 259, 345
 ———. 2003, *MNRAS*, 341, 1179
- Barth, A. J., Ho, L. C., Filippenko, A. V., & Sargent, W. L. W. 1998, *ApJ*, 496, 133
- Baugh, C. M., Cole, S., & Frenk, C. S. 1996, *MNRAS*, 282, L27
- Binney, J., & Merrifield, M. 1998, *Galactic Astronomy* (Princeton: Princeton Univ. Press), chapter 4
- Block, D. L., Stockton, A., Elmegreen, B. G., & Willis, J. 1999, *ApJ*, 522, L25
- Bloemen, J. B. G. M., et al. 1986, *A&A*, 154, 25
- Bournaud, F., & Combes, F. 2002, *A&A*, 392, 83
- Bower, G. A., Richstone, D. O., Bothun, G. D., & Heckman, T. M. 1993, *ApJ*, 402, 76
- Combes, F., & Elmegreen, B. G. 1993, *A&A*, 271, 391
- Corbelli, E., Schneider, S. E., & Salpeter, E. E. 1989, *AJ*, 97, 390
- Crothwaite, L., Turner, J. L., & Ho, P. T. P. 2000, *AJ*, 119, 1720
- Das, M., Vogel, S. N., Teuben, P. J., Regan, M. W., Sheth, K., Harris, A. I., & Jeffreys, W. H. 2003, *ApJ*, 582, 190
- de Vaucouleurs, G., de Vaucouleurs, A., Corwin, H. G., Jr., Buta, R. J., Paturel, G., & Fouqué, P. 1991, *Third Reference Catalogue of Bright Galaxies* (New York: Springer) (RC3)
- Downes, D., Reynaud, D., Solomon, P. M., & Radford, S. J. E. 1996, *ApJ*, 461, 186
- Elmegreen, B. G., Elmegreen, D. M., & Hirst, A. C. 2004, *ApJ*, 612, 191
 ———. 1985, *ApJ*, 288, 438
- Elmegreen, D. M. 1996, *IAU Colloq.* 91, *Barred Galaxies*, R. J. Buta, D. A. Crocker, & B. G. Elmegreen (San Francisco: ASP), 23
- Eskridge, P., et al. 2000, *AJ*, 119, 536
- Feldmeier, J. J., Ciardullo, R., & Jacoby, G. H. 1997, *ApJ*, 479, 231
- Ferguson, H. C., Dickinson, M., & Williams, R. 2000, *ARA&A*, 38, 667
- Ferrarese, L., et al. 1996, *ApJ*, 468, L95
- Friedli, D., & Benz, W. 1993, *A&A*, 268, 65
 ———. 1995, *A&A*, 301, 649
- Gibson, B. K., et al. 1999, *ApJ*, 512, 48
- Graham, J. A., et al. 1997, *ApJ*, 477, 535
 ———. 1999, *ApJ*, 516, 626
- Grosbol, P. J., & Patsis, P. A. 1998, *A&A*, 336, 840
- Gottzman, S. T., & Hunter, J. H., Jr. 1982, *ApJ*, 260, 65
- Hawarden, T. G., Mountain, C. M., Leggett, S. K., & Puxley, P. J. 1986, *MNRAS*, 221, P41
- Helfer, T. T., Regan, M. W., Thornley, M. D., Sheth, K., Wong, T., Vogel, S. N., Bock, D. C.-J., & Blitz, L. 2003, *ApJS*, 145, 259
- Helfer, T. T., Vogel, S. N., Lugten, J. B., & Teuben, P. J. 2002, *PASP*, 114, 350
- Herrnstein, J., Moran, J., Greenhill, L., Inoue, M., Nakai, N., Miyoshi, M., & Diamond, P. 1997, *BAAS*, 29, 1252
- Ho, L. C. 1999a, *ApJ*, 516, 672
- Ho, L. C., Filippenko, A. V., & Sargent, W. L. W. 1997, *ApJ*, 487, 591
- Ho, L. C., Ptak, A., Terashima, Y., Kunieda, H., Serlemitsos, P. J., Yaqoob, T., & Koratkar, A. P. 1999b, *ApJ*, 525, 168
- Huang, J. H., Gu, Q. S., Su, H. J., Hawarden, T. G., Liao, X. H., & Wu, G. X. 1996, *A&A*, 313, 13
- Hughes, S. M. G., et al. 1998, *ApJ*, 501, 32
- Jarrett, T. H., Chester, T., Cutri, R., Schneider, S. E., & Huchra, J. P. 2003, *AJ*, 125, 525
- Jiménez-Vicente, J., Battaner, E., Rozas, M., Castañeda, H., & Porcel, C. 1999, *A&A*, 342, 417
- Jogee, S., Scoville, N. Z., & Kenney, J. D. P. 2005, *ApJ*, 630, 837
- Jogee, S., et al. 2004, *ApJ*, 615, L105
- Karachentsev, I. D., & Tikhonov, N. A. B. 1993, *A&AS*, 100, 227
- Karachentsev, I. D., Tikhonov, N. A., Sharina, M. E., Georgiev, Ts. B., & Bilkina, B. I. 1991, *A&AS*, 91, 503
- Kenney, J. D. P. 1996a, in *ASP Conf. Ser.* 91, *Barred Galaxies*, ed. R. Buta, D. A. Crocker, & B. G. Elmegreen (San Francisco: ASP), 150
- Kennicutt, R. C., Jr. 1989, *ApJ*, 344, 685
 ———. 1998, *ARA&A*, 36, 189
- Knapen, J. H., Shlosman, I., & Peletier, R. F. 2000, *ApJ*, 529, 93
- Kormendy, J. 1993, *IAU Symp.* 153, *Galactic Bulges*, ed. H. Dejonghe & H. J. Habing (Dordrecht: Kluwer), 209
- Kormendy, J., & Kennicutt, R. C., Jr. 2004, *ARA&A*, 42, 603
- Laine, S., Shlosman, I., Knapen, J. H., & Peletier, R. F. 2002, *ApJ*, 567, 97
- Laurikainen, E., Salo, H., & Buta, R. 2004, *ApJ*, 607, 103
- Liszt, H. S., & Dickey, J. M. 1995, *AJ*, 110, 998
- Macri, L. M., et al. 1999, *ApJ*, 521, 155
- Martin, P., & Roy, J. 1994, *ApJ*, 424, 599
- Martinet, L., & Friedli, D. 1997, *A&A*, 323, 363
- Menéndez-Delmestre, K., Sheth, K., Scoville, N. Z., Jarrett, T., Schinnerer, E., Regan, M. W., & Block, D. 2004, in *Penetrating Bars through Masks of Cosmic Dust: The Hubble Tuning Fork Strikes a New Note*, ed. D. Block et al. (Dordrecht: Kluwer), 787

- Metcalfé, N., & Shanks, T. 1991, *MNRAS*, 250, 438
- Molla, M., Hardy, E., & Beauchamp, D. 1999, *ApJ*, 513, 695
- Mulder, P. S., & van Driel W. 1993, *A&A*, 272, 63
- Norman, C. A., Sellwood, J. A., & Hasan, H. 1996, *ApJ*, 462, 114
- Ohta, K., Sasaki, M., & Saito, M. 1986, *PASJ*, 38, 677
- Patrel, G., Lanoix, P., Teerikorpi, P., Theureau, G., Bottinelli, L., Gouguenheim, L., Renaud, N., & Witasse, O. 1998, *A&A*, 339, 671
- Pfenniger, D., & Norman, C. 1990, *ApJ*, 363, 391
- Planesas, P., Colina, L., & Perez-Olea, D. 1997, *A&A*, 325, 81
- Pompei, E., & Natali, G. 1997, *A&AS*, 124, 129
- Regan, M. W., Helfer, T. T., Thornley, M. D., Sheth, K., Wong, T., Vogel, S. N., Blitz, L., & Bock, D. C.-J. 2001, *ApJ*, 561, 218
- Regan, M. W., & Mulchaey, J. 1999, *AJ*, 117, 2676
- Regan, M. W., Sheth, K., & Vogel, S. N. 1999, *ApJ*, 526, 97
- Regan, M. W., & Teuben, P. J. 2003, *ApJ*, 582, 723
- . 2004, *ApJ*, 600, 595
- Rubin, V. C. 1994, *AJ*, 107, 173
- Sage, L. 1993, *A&A*, 272, 123
- Saha, A., Sandage, A., Tammann, G. A., Labhardt, L., Macchetto, F. D., & Panagia, N. 1999, *ApJ*, 522, 802
- Sakamoto, K., Okumura, S. K., Ishizuki, S., & Scoville, N. Z. 1999a, *ApJS*, 124, 403
- . 1999b, *ApJ*, 525, 691
- Sault, R. J., Teuben, P. J., & Wright, M. C. H. 1995, in *ASP Conf. Ser. 77, Astronomical Data Analysis Software and Systems IV*, ed. R. A. Shaw, H. E. Payne, & J. J. E. Hayes (San Francisco: ASP), 433
- Sellwood, J. A., & Wilkinson, A. 1993, *Rep. Prog. Phys.*, 56, 173
- Sérsic, J. L., & Pastoriza, M. 1967, *PASP*, 79, 152
- Sharina, M. E., Karachentsev, I. D., & Tikhonov, N. A. 1997, *Astron. Lett.*, 23, 373
- . 1996, *A&AS*, 119, 499
- Shen, J., & Sellwood, J. A. 2004, *ApJ*, 604, 614
- Sheth, K. 2001, Ph.D. thesis, Univ. Maryland
- Sheth, K., Regan, M. W., Scoville, N. Z., & Strubbe, L. E. 2003, *ApJ*, 592, L13
- Sheth, K., Regan, M. W., Vogel, S. N., & Teuben, P. J. 2000, *ApJ*, 532, 221
- Sheth, K., Vogel, S. N., Regan, M. W., Teuben, P. J., Harris, A. I., & Thornley, M. D. 2002, *AJ*, 124, 2581
- Shlosman, I., Frank, J., & Begelman, M. C. 1989, *Nature*, 338, 45
- Sohn, Y.-J., & Davidge, T. J. 1998, *AJ*, 115, 130
- Stetson, P. B., et al. 1998, *ApJ*, 508, 491
- Tanvir, N. R., Ferguson, H. C., & Shanks, T. 1999, *MNRAS*, 310, 175
- Thornley, M. D. 1996, *ApJ*, 469, L45
- Toomre, A. 1964, *ApJ*, 139, 1217
- Tully, R. B. 1988, *Nearby Galaxies Catalog* (Cambridge: Cambridge Univ. Press)
- Turner, J. L. 1996, in *IAU Colloq. 157, Barred Galaxies*, ed. R. Buta, D. A. Crocker, & B. G. Elmegreen (San Francisco: ASP), 146
- Turner, J. L., et al. 1998, *ApJ*, 505, 207
- van der Kruit, P. C. 1971, *A&A*, 15, 110
- Vila-Costas, M. B., & Edmunds, M. G. 1992, *MNRAS*, 259, 121
- Vogler, A., Pietsch, W., & Bertoldi, F. 1996, *Röntgenstrahlung from the Universe*, ed. H. U. Zimmermann, J. Trümper, & H. Yorke (MPE Rep. 263; Garching: MPE), 399
- Welch, W. J. 1996, *PASP*, 108, 93
- Young, J. S., & Scoville, N. Z. 1991, *ARA&A*, 29, 581
- Young, J. S., et al. 1995, *ApJS*, 98, 219
- Zaritsky, D., Kennicutt, R. C., Jr., & Huchra, J. P. 1994, *ApJ*, 420, 87
- Zhang, X. 1999, *ApJ*, 518, 613